Earth Surf. Dynam. Discuss., 1, 437–481, 2013
www.earth-surf-dynam-discuss.net/1/437/2013/
doi:10.5194/esurfd-1-437-2013

Earth Surface Dynamics Discussions
Open Access

Flocculation processes and sedimentation of fine sediments in the open annular flume – experiment and numerical modeling

I. Klassen[1], G. Hillebrand[2], N. R. B. Olsen[3], S. Vollmer[2], B. Lehmann[4], and F. Nestmann[1]

[1]Institute for Water and River Basin Management, Karlsruhe Institute of Technology, Germany
[2]Federal Institute of Hydrology, Koblenz, Germany
[3]Department of Hydraulic and Environmental Engineering, Norwegian University of Science and Technology, Trondheim, Norway
[4]Institute for Hydraulic Engineering and Water Management, Technical University Darmstadt, Germany

Received: 9 September 2013 – Accepted: 13 September 2013 – Published: 14 October 2013

Correspondence to: I. Klassen (irina.klassen@kit.edu)

Published by Copernicus Publications on behalf of the European Geosciences Union.

Abstract

The prediction of cohesive sediment transport requires numerical models which include the dominant physico-chemical processes of fine sediments. Mainly in terms of simulating small scale processes, flocculation of fine particles plays an important role since aggregation processes affect the transport and settling of fine-grained particles. Flocculation algorithms used in numerical models are based on and calibrated using experimental data. A good agreement between the results of the simulation and the measurements is a prerequisite for further applications of the transport functions.

In this work, the sediment transport model (SSIIM) was extended by implementing a physics-based aggregation process model based on McAnally (1999). SSIIM solves the Navier-Stokes-Equations in a three-dimensional, non-orthogonal grid using the k-ε turbulence model. The program calculates the suspended load with the convection-diffusion equation for the sediment concentration.

Experimental data from studies in annular flumes (Hillebrand, 2008; Klassen, 2009) is used to test the flocculation algorithm. Annular flumes are commonly used as a test rig for laboratory studies on cohesive sediments since the flocculation processes are not interfered with by pumps etc. We use the experiments to model measured floc sizes, affected by aggregation processes, as well as the sediment concentration of the experiment. Within the simulation of the settling behavior, we use different formulas for calculating the settling velocity (Stokes, 1850 vs. Winterwerp, 1998) and include the fractal dimension to take into account the structure of flocs.

The aim of the numerical calculations is to evaluate the flocculation algorithm by comparison with the experimental data. The results from these studies have shown, that the flocculation process and the settling behaviour are very sensitive to variations in the fractal dimension. We get the best agreement with measured data by adopting a characteristic fractal dimension n_{f_c} to 1.4. Insufficient results were obtained when neglecting flocculation processes and using Stokes settling velocity equation, as it is often done in numerical models which do not include a flocculation algorithm.

These numerical studies will be used for further applications of the transport functions to the SSIIM model of reservoirs of the Upper Rhine River, Germany.

1 Introduction

Suspended sediment dynamics is an important and complex field within sediment transport. Several issues may illustrate the relevance of fine, cohesive sediments: high sediment loads lead to an impairment of the flora and fauna, colmation due to fine sediments can cause a loss of habitats, and in areas with low flow velocities (e.g. at ports, in groyne fields and at barrages) sedimentation of fine-grained sediments takes place and involve cost-intensive maintenance dredging (Brunke, 1999; Winterwerp and van Kesteren, 2004; Yang, 1996). In addition, in case of contaminations, cohesive sediments may pose even more serious ecological and economic problems. Numerical modeling of the interaction between cohesive sediments, particle-bound contaminants and the water flow represents a major challenge in morphodynamics and sediment engineering.

The physical characteristics and the behavior of fine-grained sediments, that Mehta and McAnally (2007), for instance, defines as grains that are less than 63 µm in size, are affected by numerous parameters (see Fig. 1): physico-chemical factors (e.g. particle properties, particle concentration, salt content, pH-value, temperature), biological (e.g. organic matter), and flow-dependent factors (e.g. flow velocity, turbulence intensity). The sorption and adsorption processes of particle-bound contaminants on the other hand are impacted by many factors as well: e.g. organic matter content in the suspended matter, water chemistry, colloids from the water, particle and floc size (Lick et al., 1997).

A key process in cohesive sediment dynamics is the flocculation process, i.e. the possibility of primary, individual particles to form larger aggregates or flocs, composed of many small individual particles. The particle yield strength determines whether colliding particles aggregate and form larger flocs or disaggregate due to the collision-

ESURFD
1, 437–481, 2013

induced shear stress or by fluid forces, i.e. flow shear. These flocculation processes significantly alter the properties of fine-grained sediments in terms of the effective particle size, the particle density and the floc structure, expressed by the fractal dimension. It is clear that the characteristics of cohesive sediments differ strongly from the properties of coarser cohesionless particles. Consequently, numerical models which do not include a flocculation algorithm would make incorrect predictions when simulating small scale processes.

In this paper, we introduce a physics-based flocculation algorithm based on McAnally (1999), which was implemented in SSIIM 3D. SSIIM 3D is a three-dimensional numerical model solving the Navier-Stokes equations and the convection-diffusion equation for suspended sediment transport. For the calibration and testing of the algorithm we use experimental data in annular flumes (Hillebrand, 2008; Klassen, 2009). The aim of the simulation is to achieve a good agreement between the results of the simulation and the measurements as a prerequisite for further applications of the transport functions. In our simulations we model the temporal development of measured floc sizes, affected by aggregation processes, as well as the measured sediment concentration. Within the simulation of the settling behavior, we use different formulas for calculating the settling velocity (Stokes, 1850 vs. Winterwerp, 1998) and include the fractal dimension to take into account the structure of flocs. This paper aims to investigate the influence that the settling velocity formula and the floc structure have on modelling the deposition of cohesive sediments.

2 Experiments in the annular flume

2.1 Experimental set-up of the annular flume

Annular flumes are commonly used as a test rig for laboratory studies on cohesive sediments since the flocculation processes are not interfered with by pumps and an in-finite flow can be generated (Haralampides et al., 2003; Hillebrand, 2008; Krishnappan, 2006).

At the Karlsruhe Institute of Technology (KIT) in Germany there are two annular flumes with a free water surface which differ only in scale but not in their principle functioning. Both flumes consist of a rotating inner cylinder within an outer non rotating cylinder. The rotating inner cylinder generates the flow in the water column between both cylinders (see Fig. 2).

A major characteristic of the test rig are the distinct secondary currents due to the curve and the rotation of the annular flume.

For all experimental and simulation results presented in this paper one setup of boundary conditions in the small flume was used due to a reduced computation time compared to the large flume (the basin diameter of the small flume is 1.20 m, the diameter of the large flume is 3.60 m. The width of the cross sections is 0.375 m for both flumes and the water depth was kept constant at 0.28 m).

2.2 Flow field measurements and simulation in SSIIM 3D

In previous studies the hydraulic characteristics of the two test rigs have been analyzed by three-dimensional measurements using Acoustic Doppler Velocimetry and by three-dimensional numerical modeling in SSIIM 3D (Hillebrand, 2008; Hillebrand and Olsen, 2010). Experimental data on flow velocities by magnitude and flow direction as well as the turbulent kinetic energy distribution were compared with the results of the simulation. Good agreement was found for both the time-averaged flow field and the turbulence characteristics. Discrepancies were most significant in the determination of the magnitude of the turbulent kinetic energy, but general characteristics of the distribution of the TKE were the same. This is a crucial prerequisite for the further simulation of flocculation processes and sedimentation of cohesive sediments in the annular flume. A detailed description of the flow-field simulation in the annular flume is given by Hillebrand and Olsen (2010).

ESURFD

1, 437–481, 2013

2.3 Experimental method and techniques

In both annular flumes several experiments by Hillebrand and Klassen were carried out. For the calibration of the implemented flocculation algorithm, measured laboratory data from one experiment in the small flume were used (Klassen, 2009). In the experiment, the temporal development of floc sizes, affected by aggregation processes, as well as the suspended sediment concentration were measured at one point in the middle of the height of the water level (= 0.14 m) and in the middle of the flume width. The experiment was carried out in tap water. In order to simplify the complex system of natural sediments, which contain significant amounts of clay minerals as well as a certain range of organic material (Raudkivi, 1998), industrially processed Kaolinit was used. Kaolinit is a typical representative for clay minerals and is part of the mineral class of the layer silicates. In our experimental studies, the used Kaolinit had a medium grain diameter of $D_g = 2.06\,\mu m$.

For measuring the suspended sediment concentration the turbidity was recorded continuously (every 30 s) combined with taking sediment samples. In order to verify aggregation processes floc sizes were measured simultaneously using the In-Line microscope Aello 7000. All measurements were conducted at one point in the middle of the flume width. Figure 3 shows the arrangement of the measuring devices in the small flume.

The floc size measuring system Aello consists of a 38 mm wide stainless-steel pipe with a 8 mm wide slot acting as the measuring volume (see Fig. 4). On the one side of the slot the illumination devices is placed which provides the backlighting for the pictures. On the other side of the slot a microscope objective and a CCD-camera with a resolution of 1024 × 768 pixels are positioned. At the end of the stainless-steel pipe a box for camera electronics and electronic connections is located. An image recognition software analyzes the pictures and calculates characteristic parameters for particle size distributions, like the median diameter d_{50}, the particle diameter d_{16}, d_{84} or the Sauter diameter. In this paper, we use the mean diameter d_{50} as a representative pa-

ESURFD

1, 437–481, 2013

Flocculation processes and sedimentation of fine sediments

I. Klassen et al.

rameter for characterizing the particle size distribution, which is based on the diameter of approximately 1000 measured particles.

Prior to the start of the experiment, a dry amount of sediment was weighed to achieve an initial concentration of $C_0 = 500\,\mathrm{mg\,L^{-1}}$. After adding tap water, the sediment-water-suspension was mixed intensively by using a laboratory stirrer. A high stirrer frequency was used to break up possible flocs due to mixing. Before adding the sediment suspension in the annular flume, tap water was filled inside the flume to a height of 0.28 m. The sediment suspension was then added near the inner rotating cylinder to achieve a fast mixing of the suspension due to the high flow velocities and turbulence intensity at the rotating wall. The rotational frequency of the inner cylinder was set to 22 rpm (revolutions per minute). This frequency results in a horizontal velocity of approx. $0.2\,\mathrm{m\,s^{-1}}$ near the rotating boundary, decreasing to a horizontal velocity of nearly zero near the outer non rotating wall. At the beginning of the measurements a high frequency of samples was necessary due to the rapid turbidity decrease. In the further experiment the sampling was based on the degree of the turbidity decrease. Concurrently, particle sizes were measured with an interval of 15 min.

2.4 Experimental results

In Figs. 5 and 6 the measured data from the selected experiment in the small annular flume are shown. Figure 5 illustrates the measured total suspended sediment concentration presented over a time of nearly 5 h. In Fig. 6 the corresponding measured median diameter d_{50} and the d_{90} of the particles/flocs of Kaolinit can be seen over a time of 5 h with an interval of 15 min. It should be taken into account, that in fact, the experiment took about 70 h until only approx. 7 per cent of the initial sediment material was in suspension, i.e. almost the whole sediment mass deposited. However, due to the increased computation time when simulating flocculation processes over a period of 70 h, implying small time steps of a few seconds, the numerical modeling was limited to the first 5 h of the experiment.

Figure 5 shows the decrease of the initial suspended concentration from approx. $C_0 = 500\,\mathrm{mg\,L^{-1}}$ to about $C = 330\,\mathrm{mg\,L^{-1}}$ after nearly 5 h. This decrease is attributed to the deposition of the particles. In Fig. 6, the temporal development of the measured particle diameters captured by Aello, indicates flocculation processes: the first measured median particle diameter d_{50} was recorded two minutes after addition of the sediment suspension in the flume to $d_{50} = 9.3\,\mu\mathrm{m}$ ($d_{90} = 15.96\,\mu\mathrm{m}$). Since the size of the medium primary particles of Kaolinit is $D_\mathrm{g} = 2.06\,\mu\mathrm{m}$, only aggregation processes can be related to this significant increase in particle size in the order of a factor of approx. 4.5. In the time period of 5 h the maximum median floc diameter is reached after 17 min to $d_{50} = 11\,\mu\mathrm{m}$ ($d_{90} = 18.91\,\mu\mathrm{m}$), accounting for further flocculation processes. Then the median diameter is decreasing to a more or less constant value between $d_{50} = 7.5$–$8.0\,\mu\mathrm{m}$ ($d_{90} = 10.5$–$13.6\,\mu\mathrm{m}$). The decrease in floc size can be caused by the settling of the larger flocs, leaving the smaller particles in suspension. In Fig. 7 representative pictures of the particles, captured by the Aello In-Line Microscope can be seen for two measurement points: 17 min after adding the sediment suspension in the annular flume, yielding a maximum median floc size of 11 µm (left side), as well as 2.8 h after starting the experiment, resulting in a median particle diameter of 7.6 µm (right side).

The objective of this study is the numerical modeling of the measured sediment concentration and floc sizes, affected by aggregation processes, by implementing a flocculation algorithm in SSIIM 3D (flocdll) and using different settling velocity formulas (Stokes vs. Winterwerp) as well as taking into account the structure of flocs. The implemented flocculation algorithm is presented briefly in the next chapter and the applied settling velocity formulas as well as the fractal theory are introduced.

3 Flocculation algorithm in SSIIM

The flocculation algorithm was implemented in the sediment transport model SSIIM 3D (Olsen, 2011). SSIIM is an abbreviation for "Simulation of Sediment movements In

ESURFD
1, 437–481, 2013

water Intakes with Multiblock option". It is a three-dimensional numerical model solving the Navier-Stokes-Equations in a non-orthogonal grid using the k-ε turbulence model. SSIIM calculates the suspended load with the convection-diffusion equation for the sediment concentration. In previous studies, particle deposition in a laboratory flume was measured and computed in SSIIM 3D (Olsen and Skoglund, 1994). The particles were too coarse for flocculation to occur, though. In order to simulate cohesive fine sediments the software was extended by implementing a physics-based aggregation process model (Klassen et al., 2011) which is based on a calculation approach by McAnally (1999). In this paper, a short overview of the flocculation algorithm is presented below. For a detailed description in terms of the mathematical and physical aspects the reader is referred to McAnally (1999) or to Klassen et al. (2011).

The flocculation approach is based on a particle size spectrum which is described by a finite set of discrete size classes, ranging from size class $j = 1$, which contains the largest flocs/aggregates, to the size of the smallest, primary grains of class $j = s$ (see Fig. 8). Each size class has to be specified by a particle diameter and a settling velocity, respectively. Sediment mass is shifted between the size classes due to aggregation, leading to a higher sediment mass in the coarser size classes, and by disaggregation, resulting in higher sediment concentrations in the smaller size classes. The processes deposition and erosion lead to a decrease and increase of the sediment mass within each class j, respectively. The implemented flocculation algorithm allows flocculation and disaggregation of flocs due to two-body collisions caused by Brownian motion, differential settling and turbulence. Flow-induced stresses due to turbulence (no interaction of particles is necessary) may also lead to disaggregation of flocs, if these stresses exceed the particle yield strength.

Depending on a comparison between the collision-induced stresses and the yield strength of the particles several collision outcomes are possible (see Fig. 9). If both colliding particles are strong enough to resist the collision induced shear stress, these particles will aggregate (A) and form a larger floc (type 2A1). In case that the collision-induced shear stress exceeds the particle strength of one or both colliding particles, these particles will disaggregate (D). In this case, the aggregation process would result in either 2 (type 2D2) or 3 particles (type 2D3).

Since cohesive forces between fine sediments are strong, it is assumed in this study that every particle collision results in a bond at the point of contact, i.e. the collision efficiency was set to 1. However, since the collision efficiency depends on the sediment characteristics, it should be noted, that this sediment parameter could differ from the value of 1. For a detailed analysis a sensitivity study regarding the collision efficiency would be appropriate.

Flocculation processes do not alter only the properties of fine-grained sediments in terms of the effective particle size, but also have an impact on the floc structure, expressed by the fractal dimension. The structure of flocs is a key factor when simulating flocculation processes since it determines the floc density, the particle yield strength and the collision-induced shear stresses which in turn influence the settling velocity and the aggregation mechanism. In previous sensitivity analyses, realized by adopting a simple test case in a stagnant water column in SSIIM 3D, the aggregation processes to variations in fractal dimensions were studied (Klassen et al., 2011). It could be shown that the fractal dimension has a major impact on the overall mass settling. Thus, the fractal dimension should be taken into account for modeling the experiments in a physically correct way. In the next chapter, first the main concept of fractal theory of floc structure is presented shortly and the applied values for the fractal dimension for the numerical simulation are given.

3.1 Fractal theory of floc structure and application to the numerical model

The main concept of fractal theory is the self-similarity of the floc structure, i.e. the fact that a growing entity shows the same structure as at its initial state (Mandelbrot, 1982). Therefore, growing fractals are treated as scale-invariant objects (Vicsek, 1992). Real fractal structures are an idealization, since every geometrical body has a smallest and largest dimension (Khelifa and Hill, 2006; Nagel, 2011). In spite of this limitation several

ESURFD
1, 437–481, 2013

models use the approach of fractal structures in order to characterize the properties of flocs.

The floc structure (expressed by the fractal dimension n_f) has an impact on the floc density, the particle yield strength and the collision-induced shear stresses. The floc density in turn influences the settling velocity, thus the deposition of fine particles. The particle yield strength in connection with the collision-induced shear stresses determine if two colliding particles aggregate or disaggregate due to the collision-induced shear stresses, meaning that the fractal dimension influences the aggregation mechanism as well.

The fractal dimension decreases from the value $n_f = 3.0$ for small and compact particles with particle sizes close to the primary particles to about $n_f = 1.0$ for large and irregular flocs with an open and porous structure, as indicated in Fig. 10. For example, if the flocs are connected on one line, the fractal dimension is about 1, while if they are on a flat plane, the dimension is 2. And a snowflake with equal distribution in all three spatial directions would have a value of about 3.

The smaller the fractal dimension is, the smaller is the floc density, the particle strength and the collision-induced stresses. Applying the fractal theory to a settling velocity formula is the main difference compared to Stokes' settling relation (1850), which treats particles as solid Euclidean spheres with $n_f = 3.0$.

Numerical models, including the fractal dimension, often consider an overall constant value for n_f for the whole floc size spectrum (Kranenburg, 1999; Xu et al., 2008). These models often assume an average value for the fractal dimension such as $n_f = 2.0$.

However, several previous studies proposed the concept of a variable fractal dimension since they showed improvements in predicting the floc size distribution and the floc settling velocity (Khelifa and Hill, 2006; Maggi, 2007; Son and Hsu, 2008). The suggestion of including a variable fractal dimension is based on the idea that there is a transition during the growth from the smaller Euclidean, primary particles to larger real fractal aggregates. This leads to a decrease of the fractal dimensions as floc sizes are increasing (Maggi, 2007). According to this theory, primary particles should have a

ESURFD
1, 437–481, 2013

value of $n_f = 3.0$, whereas large flocs should have fractal dimensions of about $n_f = 2.0$ and smaller. Once the flocs have reached a certain size, they can be treated as real fractals. The value of their fractal dimension is constant and depends only on the flow conditions or the particle concentration. Two ranges of behavior were observed in regards to the fractal dimension of flocs at a constant turbulent shear rate by Kumar et al. (2010). In the first region, for floc sizes less than 200 µm, a variable fractal dimension was needed to describe the submerged specific gravity as a function of floc size. In the second region, for floc sizes greater than 200 µm, a constant fractal dimension was found to suffice in describing the submerged specific gravity. The constant fractal dimension for this second region was $n_f = 2.3$ for fresh water flocs and $n_f = 1.95$ for salt water flocs (Kumar et al., 2010).

In this paper we used the formula for the variable fractal dimension based on previous studies of Khelifa and Hill (2006). They proposed a power law to describe the variable fractal dimension which depends on the floc size D_j and the primary particle size D_g:

$$n_f = \alpha \cdot \left(\frac{D_j}{D_g}\right)^{\beta} \tag{1}$$

with $\alpha = 3$ and

$$\beta = \frac{\log(n_{f_c}/3)}{\log(D_{f_c}/D_g)} \tag{2}$$

where n_{f_c} represents a characteristic fractal dimension and D_{f_c} a characteristic floc size. Khelifa and Hill recommend the typical value for n_{f_c} and D_{f_c} to be $n_{f_c} = 2.0$ and $D_{f_c} = 2000$ µm, if they are not measured or calculated. However, they also showed that the predicted effective density is very sensitive to the parameter n_{f_c}. The magnitude of the fractal dimension depends on the mechanism by which aggregates grow. Flocs formed by particle–cluster aggregation have fractal dimensions higher than those formed by cluster–cluster aggregation, even if they are of the same size. Thus, in case of uncertainty regarding the characteristic values, the range of n_{f_c} has to be considered in models describing flocculation processes. In this study, several values for the characteristic fractal dimension n_{f_c} were applied to take into account the effect of variations of n_{f_c} on the aggregation processes: n_{f_c} = 1.4, 1.7, 2.0, 2.3 and 2.6. According to the measured mean particle diameters d_{50} shown in Fig. 6, we set the value for the characteristic floc size D_{f_c} randomly to 15 µm.

Figure 11 illustrates the impact of the value of the characteristic fractal dimension n_{f_c} on the range of the effective fractal dimension n_f. Adopting n_{f_c} to 1.4 yields a size dependent fractal dimension in the range between n_f = 3.0 for the primary particles of size 2.06 µm to n_f of about 1.0 for larger flocs in the range of 30–50 µm (blue curve). In contrast, applying n_{f_c} = 2.6 results in much more compact aggregates, since the fractal dimension for a particle size spectrum between 2.06–50 µm is between 3.0 and 2.4 (red line). These significant differences in floc structure due to various fractal dimensions are indicated qualitatively by the pictures of the flocs, showing rather fragile flocs for n_{f_c} = 1.4 and more dense aggregates for n_{f_c} = 2.6.

3.2 Settling velocity formula

As shown in the previous chapter, fractal flocs can be characterized by their floc size, their structure and their density. These properties in turn are influenced by the flow conditions (turbulence) or by the sediment characteristics, like the sediment concentration or the cohesion of the particles. Accordingly, the settling velocity of flocs can be calculated depending on many factors.

In order to take into account that aggregates are fractal entities, we use the settling velocity formula based on Winterwerp (1998). In this equation the floc structure is accounted for by using the fractal dimension to compute the effective density $\Delta\rho_j$ of each particle size class D_j. The effective density $\Delta\rho_j$ results from the difference between the density of each particle size class, ρ_j and the fluid density ρ_W = 1000 kg m^{-3}. The density of each particle size class, ρ_j, is determined by the following equation (McAnally and Mehta, 2000):

$$\rho_j = \text{smaller of} \begin{cases} \rho_g \\ \rho_W + B_\rho \cdot \left(\dfrac{D_g}{D_j}\right)^{3-n_f} \end{cases} \tag{3}$$

where ρ_g = grain density of primary particles (set to 2650 kg m^{-3}); ρ_W = fluid density (=1000 kg m^{-3}); B_ρ = an empirical sediment- and flow-dependent density function. For sediment in still water B_ρ becomes to 1650 kg m^{-3}; D_g = primary grain diameter and n_f = fractal dimension (= 1.0 to 3.0).

Hence, by deriving a balance of forces between the drag force and the lift force, the settling velocity formula $W_{S,j}$ by Winterwerp (1998) in still water becomes:

$$W_{S,j}(\text{Winterwerp}) = \frac{\alpha}{\beta} \cdot \frac{D_j^2}{18\nu} \cdot g \cdot \frac{\Delta\rho_j}{\rho_W} \tag{4}$$

where α, β = particle shape coefficients. For spherical ($\alpha = \beta = 1$), solid Euclidean particles, i.e. $n_f = 3.0$, the equation reduces to a standard Stokes settling relation, which does not consider the fractal dimension (Stokes, 1850):

$$W_{S,j}(\text{Stokes}) = \frac{D_j^2}{18\nu} \cdot g \cdot \frac{\rho_g - \rho_W}{\rho_W} \tag{5}$$

We compare the results using the implemented flocculation algorithm in combination with the settling velocity by Winterwerp (1998) with the results obtained by excluding flocculation processes and using Stokes' (1850) settling velocity which does not consider the fractal structure.

The simulation results in terms of applying various characteristic fractal dimensions n_{f_c} and using the settling velocity formula based on Winterwerp are presented in the next chapter. Afterwards, the results by neglecting the flocculation processes of cohesive sediments and adopting Stokes settling velocity are illustrated.

ESURFD
1, 437–481, 2013

4 Simulation results and discussion

4.1 Number of size classes and initial conditions

Modeling flocculation and fragmentation processes requires the definition of a discrete number of size classes and the corresponding particle sizes. In this study a size class-based model (SCB) was used to describe the particle size spectrum (Maerz et al., 2011; Verney et al., 2011). The SCB model is based on the population equation system that describes the floc population in N discrete size classes. Each of the used N discrete size classes corresponds to a specific particle size D_j and a related particle mass M_j, where the particle mass of each size class is determined from the density, assuming that all particles are spherical (McAnally, 1999):

$$M_j = \frac{D_j^3 \pi \rho_j}{6} \quad (6)$$

The density ρ_j in turn is calculated depending on the fractal dimension (see Eq. 3). Each particle mass, M_j, is represented by a mass class interval, which contains particles with the smallest particle mass M_j(lower) and the largest particle mass M_j(upper) of this class. Based on a linear mean formulation of M_j, the mass class interval is calculated by (McAnally, 1999):

$$M_j(\text{upper}) = \frac{M_j + M_{j-1}}{2} \text{ with } M_j(\text{upper}) = M_{j-1}(\text{lower}) \quad (7)$$

The particle sizes are logarithmically distributed starting from the smallest primary particle diameter D_g to the maximum floc size D_max by using the following equation (Maerz et al., 2011):

$$D_j = D_\mathrm{g}^{1+(i-1)/(N-1)\cdot(\log_{10}(D_\mathrm{max})/\log_{10}(D_\mathrm{g})-1)} \quad (8)$$

ESURFD
1, 437–481, 2013

Flocculation processes and sedimentation of fine sediments

I. Klassen et al.

In this study $N = 10$ size classes were defined. According to the size of the primary particles of Kaolinit in the experiment the minimum diameter was set to $D_g = 2.06\,\mu m$. The maximum floc size was defined based on the measured floc sizes, captured by Aello. In Fig. 12 all measured flocs sizes within the first 5 h of the experiment are shown.

Most particles were found in the range between 4 and 10 µm. Due to the limitations of the image recognition software, the smallest particle sizes were detected to about 4 µm (it should be noted that probably smaller particles were in suspension which could not be detected by the software), however the largest flocs have a size in the range between 30–50 µm. Hence, the coarsest particle size class was set to $D_{max} = 35\,\mu m$, which is related to a specific particle mass, thus to a mass class interval. The largest particle mass $M_{j,(upper)}$ of this class corresponds to the maximum measured floc size of 50 µm. In Table 1 the chosen particle size classes ($N = 10$) for the numerical model in SSIIM 3D are listed, as well as the initial concentration C_0 in each size class, which was defined randomly to achieve an initial total concentration of $C_0 = 500\,mg\,L^{-1}$. A different choice of initial concentrations C_0 in the size classes would result in a different initial floc size. However, Son and Hsu (2008), for example, observed that the initial floc size affects only the time to reach the equilibrium state, but not the final (equilibrium) floc size. Son and Hsu (2008) have shown, that their model results are insensitive to this uncertainty as far as the final floc size is concerned.

4.2 Simulated concentrations and median floc diameters due to variations in fractal dimension

In Figs. 13 and 14 the results from the numerical simulations adopting different values for the characteristic fractal dimension n_{f_c} ($D_{f_c} = 15\,\mu m$ is constant for all calculations) are shown. The settling velocity by Winterwerp was used for all analyses.

Figure 13 illustrates the total concentration development of the measured values (red, jagged line) and the simulated curves by conducting a sensitivity analyses in terms of the characteristic fractal dimension n_{f_c}, resulting in various fractal dimensions

ESURFD
1, 437–481, 2013

n_f (cf. Fig. 11). Both the experiment and simulation results, that are shown in the graph are recorded at the same point in the annular flume (in the middle of one cross section, at the half of the water depth).

First of all it can be seen in Fig. 13 that the simulation is very sensitive to different characteristic fractal dimensions. The concentrations are decreasing faster by adopting higher values of n_{f_c}, resulting in higher fractal dimensions n_f. These results seem reasonable due to the fact that the floc density increases with higher values of n_f (see Eq. 3), causing a higher settling velocity. Higher settling velocities in turn lead to a faster deposition of the sediment mass. Adopting the characteristic fractal dimension to $n_{f_c} = 1.4$ yields the best agreement with the measured data, since the slope of the concentration curve is less steep as for the other simulations.

Nevertheless, the initial decrease of the concentration as it is indicated in the experiment is not simulated in the same way by any of the simulation results. Here, a sensitivity analysis of the initial conditions could bring an improvement. One factor resulting in a stronger decrease of the concentration could be that a certain portion of the particles (the coarser ones), added initially in the annular flume, do not exhibit fractal structures and settle down as near-solid Euclidean spheres with $n_f \approx 3.0$, causing a faster initial decrease of the concentration. In the model this could be implemented by defining size classes, that do not have fractal structures and are excluded from the flocculation process. This issue should be verified for the next simulations.

In the case of $n_{f_c} = 1.4$, the range of the fractal dimension n_f in the simulation is between 1.0 and 3.0 for the detected particle size spectrum. However, most of the aggregates, which are larger than 15 µm, would imply a fractal dimension of 1.4 and lower, meaning that these aggregates have an open and fragile structure.

Although deviations between experiment and simulation were found in respect of the initial concentration decrease, it could be shown that the simulation is very sensitive to the fractal dimension and tendencies in the concentration evolution are similar by using a characteristic fractal dimension of 1.4. The development of the corresponding

ESURFD

1, 437–481, 2013

simulated median diameters d_{50} confirms that agreement is best by setting n_{f_c} to 1.4 as it is shown in Fig. 14.

In Fig. 14, the respective calculated median diameter is presented over 5 h. The red line represents the data from the experiments, the other lines are the simulation results by using different characteristic fractal dimensions. In the experimental results, the peak of the median floc diameter (11 µm), 17 min after adding the sediment suspension in the annular flume indicates flocculation. Then a decrease of the median diameter follows which is probably caused by the deposition of the larger particles. This increase in floc size followed by a decrease in aggregate size appears for all calculation results. Thus, in general, aggregation processes are simulated for all cases (Sect. 4.3 shows the simulated flocculation process for $n_{f_c} = 1.4$ in detail, illustrated by the shifting of particle mass between the size classes).

In Fig. 14, the value of the characteristic fractal dimension determines the maximum floc size, the time to achieve the maximum floc size and the slope following the peak. The best result is based on a characteristic value $n_{f_c} = 1.4$. For $n_{f_c} = 1.4$, the median diameter is increasing, as aggregation processes take place, to a maximum value of 9.5 µm and then is decreasing slightly. For $n_{f_c} = 2.6$ the maximum median diameter is 18 µm. Then, the median particle size is also decreasing, but the slope is much steeper compared to $n_{f_c} = 1.4$. The higher maximum median diameter for $n_{f_c} = 2.6$ can be attributed to the more flow resistant particles, resulting from higher fractal dimensions. Adopting $n_{f_c} = 2.6$ leads to more compact particles/flocs, which are not broken up by flow-induced stresses that easily compared to weak particles with lower fractal dimensions. Large and weak flocs ($n_{f_c} = 1.4$) disaggregate due to flow-shear and lead to a shifting of particle mass in the smaller size classes (see Sect. 4.3). In the case of $n_{f_c} = 2.6$ not all flocs of the same size as for $n_{f_c} = 1.4$ disaggregate due to their more compact structure. Thus, the shifting in smaller size classes due to disaggregation caused by flow-induced stresses, is not that significant. This results in a larger maximum median diameter. The steeper slope of the d_{50} for $n_{f_c} = 2.6$ is caused by the higher density of the compact particles, leading to a faster decrease of these particles.

ESURFD
1, 437–481, 2013

Differences are also found in terms of the time to achieve the maximum floc diameter. While this measured median diameter is detected 17 min after adding the suspension in the flume, the calculated maximum floc diameter is reached after about 1.2 h for $n_{f_c} = 1.4$ (for $n_{f_c} = 2.6$ after 1.3 h), decreasing afterwards slower than in the experiment. In spite of these deviations it can be summarized that adopting a characteristic fractal dimension of $n_{f_c} = 1.4$ and using the settling velocity based on Winterwerp we get the best agreement with the measured data. The flocculation process, which is shown in particular in the next chapter, can be simulated and gives plausible results. Excluding these flocculation processes and using the settling velocity based on Stokes would give poor results in comparison to the measured data (see Sect. 4.4).

4.3 Simulated flocculation processes by shifting of particle mass through the size classes

The flocculation process is realized by shifting mass through the size classes. Using the most appropriate value for the characteristic fractal dimension $n_{f_c} = 1.4$ ($D_{f_c} = 15\,\mu$m) results only in the aggregation type 2A1, i.e. two colliding particles are always strong enough to resist the collision induced shear stress and form larger aggregates. Disaggregation is only caused by flow-induced stresses, which lead to a break-up of the weakest particles of size class 1, 2, 3 and 4 (for example, adopting $n_{f_c} = 2.6$ would cause disaggregation by flow-induced stresses only of size class 1). These particles have a fractal dimension n_f in the range between $n_f = 1.0$–1.5, meaning that these aggregates have a porous and fragile structure. Figure 15 shows the temporal development of the concentrations of each size class. The decrease of the concentration of the smaller size classes 7, 8, 9 and 10 and the shifting of mass into the larger particle size classes 4, 5 and 6 illustrate the aggregation of type 2A1. Size class 1 and 2 are immediately destroyed by the flow shear, resulting in an abrupt decrease of the concentration in the first few seconds and in a shifting of the concentration in the smaller size classes. Particle size class 3 and 4 will also break up due to fluid forces, but concurrently mass is shifted in these classes by the aggregation processes of the smaller

ESURFD
1, 437–481, 2013

aggregates resulting in an increase of the concentrations. Hence, in Fig. 15 the shifting of concentrations has to be interpreted as a result of flocculation processes, break-up due to fluid shear, as well as simultaneously occurring deposition. These processes overlap, but dominant mechanisms can be estimated over time. It can be seen that the flocculation process is most significant for about the first hour of the simulation similar to the experiment. Afterwards aggregation processes further occur, but the deposition of the sediment material dominates then.

4.4 Simulation results obtained by excluding flocculation processes and using the settling velocity based on Stokes

Figures 16 and 17 show the results obtained by excluding flocculation processes and using the well-known settling velocity formula based on Stokes (1850), which does not consider the fractal nature of flocs. It is a commonly used method for calculating settling velocities of fine sediments in numerical models which do not include a flocculation algorithm.

In Fig. 16, again the measured concentration (red line) as well as the simulated concentrations (blue and green lines) over a time period of 5 hours are shown. The blue line represents the above mentioned results using a characteristic fractal dimension of 1.4. The green line is calculated when the flocculation algorithm is not used in the numerical model and the settling velocity based on Stokes is adopted, while all other settings are identical. Figure 17 illustrates the corresponding median diameter d_{50} over time. It can be seen that the concentration is decreasing much faster when excluding flocculation processes and using Stokes, yielding insufficient results in comparison to the measured data. We get insufficient results with respect to the median diameter as well (see Fig. 17). If no aggregation processes occur, the aggregates settle down as individual particles, which results in a more abrupt decrease of the median diameter due to the deposition of the larger particles leaving the smaller ones in suspension.

Although the calculated median diameter d_{50} is much smaller by using Stokes than the one based on Winterwerp, the corresponding concentration is decreasing faster

ESURFD
1, 437–481, 2013

illustrating the impact of the floc structure on the settling velocity. Using Stokes' settling velocity implies that all particles are treated as solid Euclidean particles, i.e. $n_f = 3.0$, including a density of $\rho_g = 2650\,\mathrm{kg\,m^{-3}}$. By contrast, adopting Winterwerp's approach and considering the fractal dimension yields a decreased density with increasing floc sizes. Thus, for the same particle size the settling velocity based on Stokes is much higher than using Winterwerps' equation, as indicated in Fig. 18. In particular, these differences become larger for large flocs with a porous and fragile structure represented by lower fractal dimensions.

The significantly higher settling velocities based on Stokes are responsible for the stronger decrease of the sediment mass. It can be seen, when excluding flocculation processes and using the well-known Stokes' settling equation, we get insufficient results using the same initial grain size distribution. A better agreement with the measured data could be achieved by lower sedimentation rates. This would require even finer particles which in turn would not conform with the measured data. The simulation results show that taking into account flocculation processes and using a settling velocity formula which considers a reduced density yields better results than excluding aggregation mechanisms. In this study, taking into account the used clay mineral Kaolinit and the chosen hydraulic flow conditions, the implemented flocculation algorithm achieves the best results for a characteristic fractal dimension of $n_{f_c} = 1.4$ and for a characteristic floc size of $D_{f_c} = 15\,\mu\mathrm{m}$. In the future work the calibration of the algorithm has to be optimized by sensitivity analyses in terms of the initial conditions of the numerical calculation. Aside from the initial conditions of the simulation also boundary conditions in terms of modeling simultaneously occurring erosion could be checked. For the sake of simplicity the erosion process was neglected in these numerical studies. For the next numerical simulations potential resuspension of deposited particles could be included. The calculation of erosion would result in a slower decrease of the sediment mass which would corresponds more to the measured data.

ESURFD
1, 437–481, 2013

5 Conclusions and application

In this study experimental data from studies in annular flumes (Hillebrand, 2008; Klassen, 2009) were used to test and calibrate a flocculation algorithm in SSIIM 3D, which is based on McAnally (1999). Both measured floc sizes as well as the sediment concentration of the experiment were modeled over a time period of the first 5 h of the experiment. Within the simulation, in order to take into account the fractal structure of flocs, we included the fractal dimension and used the settling velocity formula based on Winterwerp (1998), which accounts for a lower density with increasing floc size. The fractal dimension decreases from the value $n_f = 3.0$ for small and compact particles to about $n_f = 1.0$ for large and fragile flocs. In our study a variable size-dependent fractal dimension was considered, expressed as a function of floc and primary particle size, and which also depends on a characteristic fractal dimension n_{f_c} and a characteristic floc size D_{f_c} (Khelifa and Hill, 2006). The sensitivity of the flocculation process to the parameter n_{f_c} was studied by adopting different values for this parameter ($n_{f_c} = 1.4$, 1.7, 2.0, 2.3 and 2.6) and setting the characteristic floc size D_{f_c} constant to 15 µm. The simulation results show that the flocculation process and the settling behaviour is very sensitive to variations in the fractal dimension:

- The higher the fractal dimension of the particles/flocs is, i.e. the more dense and compact the particles are, the faster the concentration is decreasing.

- Adopting Winterwerp's formula for the settling velocity, we get the best agreement with the measured concentration for $n_{f_c} = 1.4$, indicating that many flocs exhibit an open and porous structure.

- The temporal evolution of the simulated median diameter d_{50} yields also the best result for $n_{f_c} = 1.4$.

However, the initial decrease of the concentration as it is indicated in the experiment could not be simulated in the same way by any of the simulation results. Here, further

ESURFD
1, 437–481, 2013

sensitivity analyses in terms of the initial and boundary conditions would bring an improvement and optimize the calibration of the flocculation algorithm. It could be shown that in general the flocculation algorithm gives reasonable results and flocculation processes can be modeled in a physically plausible way.

The results using the settling velocity by Winterwerp (1998) and taking into account the floc structure were compared with the results obtained by excluding flocculation processes and using Stokes' (1850) settling velocity which does not consider the floc structure. It could be shown, that we get insufficient results when neglecting flocculation processes and using Stokes while accounting for both concentration and grain size evolution.

The next step of our study is the validation of this calculations by further annular flume experiments. In this study the calibration was carried out by laboratory data in the small annular flume. Further experimental data in the large annular flume provide the opportunity for model validation. Finally, these results should find application in a numerical model simulating cohesive processes in nature: the flocculation algorithm will be used for further applications of the transport functions to the SSIIM model of reservoirs of the Upper Rhine River, Germany. In-situ measurements of the floc sizes will be used as input data for the numerical model of the barrage Iffezheim, as one of the reservoirs. At the Iffezheim barrage deposition of fine-grained sediments and particle-bound contaminants leads to an environmental risk and involve great economic concern. Sedimentation rates of about 115 000 m^3 per year are leading to a high amount of material that has to be dredged (Köthe et al., 2004). In the longer term, our objective is to use the implemented flocculation algorithm in combination with particle-bound and solved contaminants for modeling the suspended and contaminant transport for the Iffezheim reservoir.

Acknowledgements. The study is supported by the Federal Institute of Hydrology, Germany in the framework of the cooperation project "Experimental and numerical studies of the interaction between cohesive sediments, particle-bound contaminants and the water flow".

References

Brunke, M.: Colmation and depth filtration within streambeds: Retention of particles in hyporheic interstices, Int. Rev. Hydrobiol., 84, 99–117, 1999.

Haralampides, K., McCorquodale, J. A., and Krishnappan, B. G.: Deposition Properties of Fine Sediment, J. Hydraul. Eng.-ASCE, 129, 230–234, 2003.

Hillebrand, G.: Transportverhalten kohäsiver Sedimente in turbulenten Strömungen – Untersuchungen im offenen Kreisgerinne, Ph.D. thesis, Universität Karlsruhe (TH), Germany, 2008.

Hillebrand, G. and Olsen, N. R. B.: Hydraulic Characteristics of the Open Annular Flume – Experiment and Numerical Modeling. The first European Congress of the IAHR, 4–6 May 2010, Edinburgh, 2010.

Hillebrand, G., Klassen, I., Olsen, N. R., and Vollmer, S.: Modelling fractionated sediment transport and deposition in the Iffezheim reservoir, 10th International Conference on Hydroinformatics, Hamburg, Germany, 2012.

Khelifa, A. and Hill, P. S.: Models for effective density and settling velocity of flocs, J. Hydraul. Res., 44, 390–401, 2006.

Klassen, I.: Absinkverhalten kohäsiver Sedimente in turbulenten Strömungen – Ermittlung von Skalierungseffekten der Versuchseinrichtung Kreisgerinne, Diplomathesis, Universität Karlsruhe (TH), Germany, 2009.

Klassen, I., Hillebrand, G., Olsen, N. R., Vollmer, S., Lehmann, B., and Nestmann, F.: Modeling fine sediment aggregation processes considering varying fractal dimensions, Proceedings of the 7th IAHR Symposium on River, Coastal and Estuarine Morphodynamics, 6–8 September 2011, Beijing, China, 2011.

Köthe, H., Vollmer, S., Breitung, V., Bergfeld, T., Schöll, F., Krebs, F., and v. Landwüst, C.: Environmental aspects of the sediment transfer across the Iffezheim barrage, River Rhine, Germany, Proceedings of WODCON XVII, Hamburg, 2004.

Kranenburg, C.: Effects of floc strength on viscosity and deposition of cohesive sediment suspensions, Cont. Shelf Res., 19, 1665–1680, 1999.

Krishnappan, B. G.: Cohesive sediment transport studies using a rotating circular flume, The 7th International Conference on Hydroscience and Engineering (ICHE-2006), 10–13 September, Philadelphia, USA, 2006.

Kumar, R. G., Strom, K. B., and Keyvani, A.: Floc properties and settling velocity of San Jacinto estuary mud under variable shear and salinity conditions, Cont. Shelf Res., 30, 2067–2081, 2010.

Lick, W., Chroneer, Z., and Rapaka, V.: Modeling the dynamics of the sorption of hydrophobic organic chemicals to suspended sediments, Water Air Soil Poll., 99, 225–235, 1997.

Maerz, J., Verney, R., Wirtz, K., and Feudel, U.: Modeling Flocculation processes: Intercomparison of a size class-based model and a distribution-based model, Cont. Shelf Res., 31, S84–S93, 2011.

Maggi, F.: Variable fractal dimension: A major control for floc structure and flocculation kinematics of suspended cohesive sediment, J. Geophys. Res., 112, C07012, doi:10.1029/2006JC003951, 2007.

Mandelbrot, B. B.: The fractal geometry of nature, Freeman, New York, 1982.

McAnally, W. H.: Aggregation and deposition of fine estuarial sediment, Ph.D. thesis, Univ. of Fla., Gainesville, Fla., 1999.

McAnally, W. H. and Mehta, A. J.: Aggregation rate of fine sediment, J. Hydraul. Eng., 126, 883–892, 2000.

Mehta, A. J. and McAnally, W. H.: Fine-Grained Sediment Transport, in: Sedimentation Engineering: Processes, Measurements, Modeling and Particle. ASCE Manuals and Reports on Engineering Practice No. 110, edited by: Garcia, M. H., Published by American Society of Civil Engineers, 2007.

Nagel, M.: Zur inneren Morphogenese von Flocken mittels Clusteranalyse, Ph.D. thesis, Technische Universität Cottbus, Germany, 2001.

Olsen, N. R. B.: A three-dimensional numerical model for Simulation of Sediment movements In water Intakes with Multiblock option. Version 1 and 2. User's manual, Department of Hydraulic and Environmental Engineering, The Norwegian University of Science and Technology, Trondheim, Norway, 2011.

Olsen, N. R. B. and Skoglund, M.: Three-dimensional numerical modeling of water and sediment flow in a sand trap, J. Hydraul. Res., 32, 833–844, 1994.

Raudkivi, A. J.: Loose Boundary Hydraulics, A.A. Balkema, Rotterdam, Netherlands, 1998.

Son, M. and Hsu, T.-J.: Flocculation model of cohesive sediment using variable fractal dimension, Environ. Fluid Mech., 8, 55–71, 2008.

Stokes, G. G.: On the Effect of the Internal Friction of Fluids on the Motion of Pendulums, From the Transactions of the Cambridge Philosophical Society, Vol. IX, 1850.

ESURFD

1, 437–481, 2013

Flocculation processes and sedimentation of fine sediments

I. Klassen et al.

Verney, R., Lafite, R., and Brun-Cottan, J.: Behaviour of a floc population during a tidal cycle: laboratory experiments and numerical modelling, Cont. Shelf Res., 31, S64–S83, 2011.
Vicsek, T.: Fractal Growth Phenomena, World scientific, Singapore, 1992.
Winterwerp, J. C.: A simple model for turbulence induced flocculation of cohesive sediment, J. Hydraul. Res., 36, 309–326, 1998.
Winterwerp, J. C. and Van Kesteren, W. G. M.: Introduction to the physics of cohesive sediment in the marine environment, in: Developments in sedimentology, Vol. 56, Elsevier, New York, 2004.
Xu, F., Wang, D. P., and Riemer, N.: Modeling flocculation processes of fine-grained particles using a size-resolved method: Comparison with published laboratory experiments, Cont. Shelf Res., 28, 2668–2677, 2008.
Yang, C. T.: Sediment Transport: Theory and Practice, McGraw-Hill series in water resources and environmental engineering, 1996.

ESURFD
1, 437–481, 2013

Flocculation processes and sedimentation of fine sediments

I. Klassen et al.

Table 1. Chosen particle size classes ($N = 10$) and initial concentration C_0 for each size class for the numerical model in SSIIM 3D. Each size class is represented by a mass class interval $M_{j,\text{upper}}$ and $M_{j,\text{lower}}$.

Size class	1	2	3	4	5	6	7	8	9	10
Particle size (µm)	35	25.5	18.7	13.6	9.9	7.3	5.3	3.9	2.8	2.06
C_0 (mg L^{-1}); $\sum = 500$ mg L^{-1}	25	25	20	20	25	25	65	125	120	50

ESURFD
1, 437–481, 2013

Flocculation processes and sedimentation of fine sediments

I. Klassen et al.

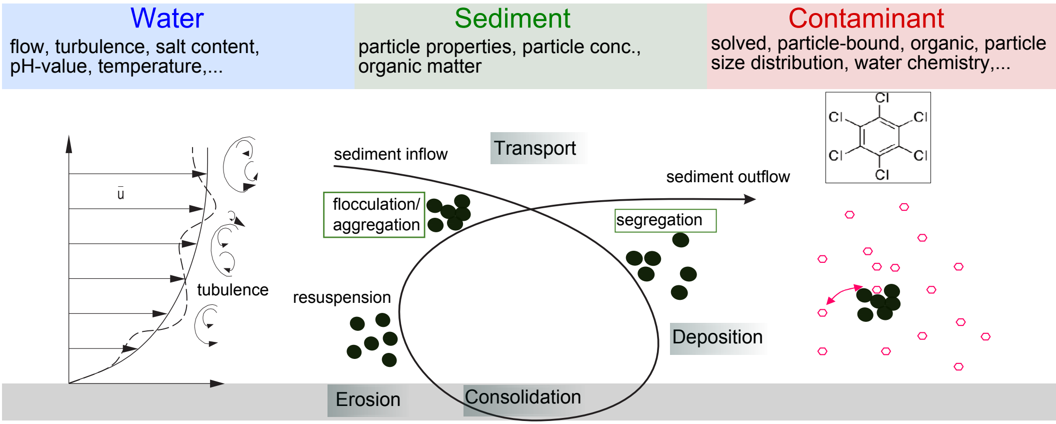

Fig. 1. Factors influencing cohesive sediment transport.

ESURFD
1, 437–481, 2013

Flocculation processes and sedimentation of fine sediments

I. Klassen et al.

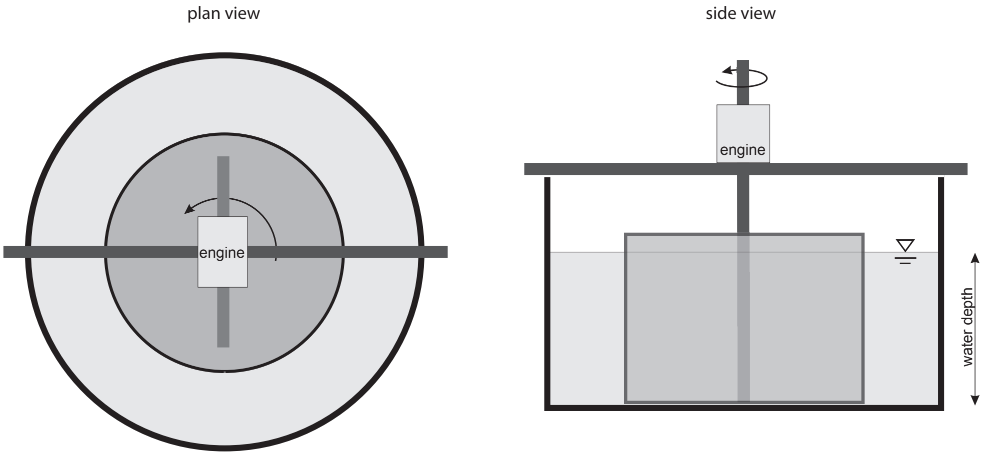

Fig. 2. Simplified sketch of the open annular flume (Hillebrand and Olsen, 2010).

ESURFD
1, 437–481, 2013

Flocculation processes and sedimentation of fine sediments

I. Klassen et al.

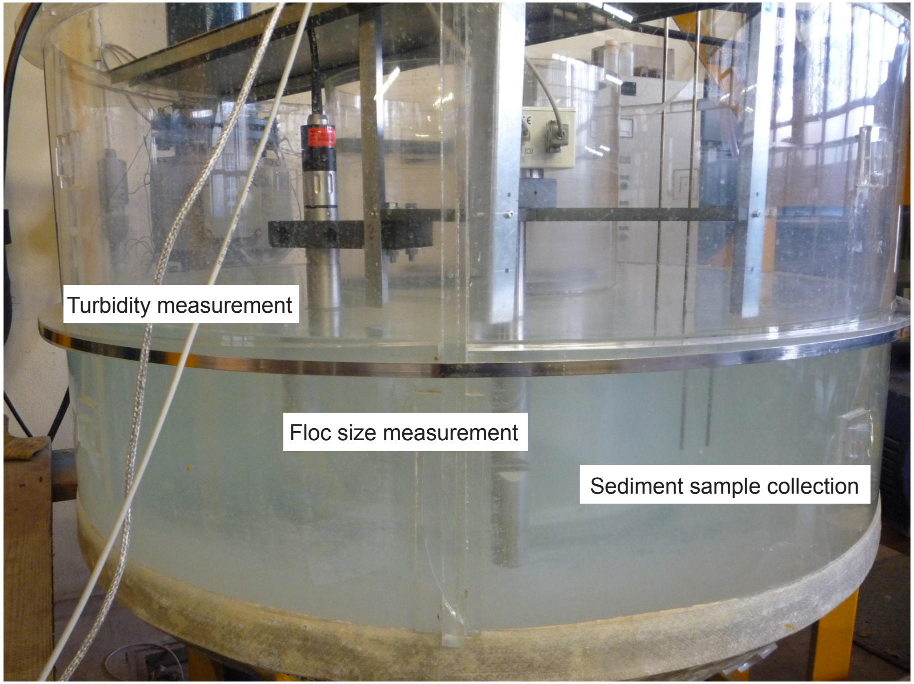

Fig. 3. Arrangement of the measuring devices in the small flume.

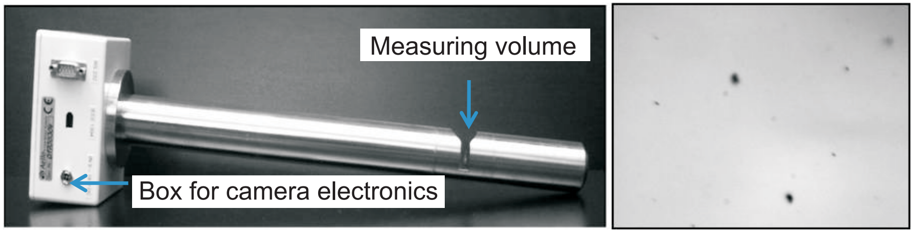

Fig. 4. Aello In-Line Microscope.

ESURFD
1, 437–481, 2013

Flocculation processes and sedimentation of fine sediments

I. Klassen et al.

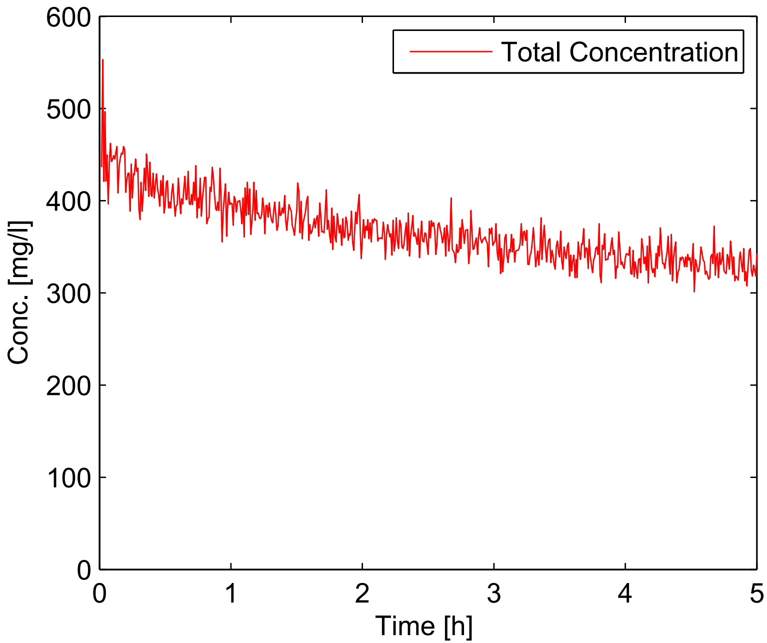

Fig. 5. Measured suspended sediment concentration over a time of approx. 5 h at the center of the cross section.

ESURFD
1, 437–481, 2013

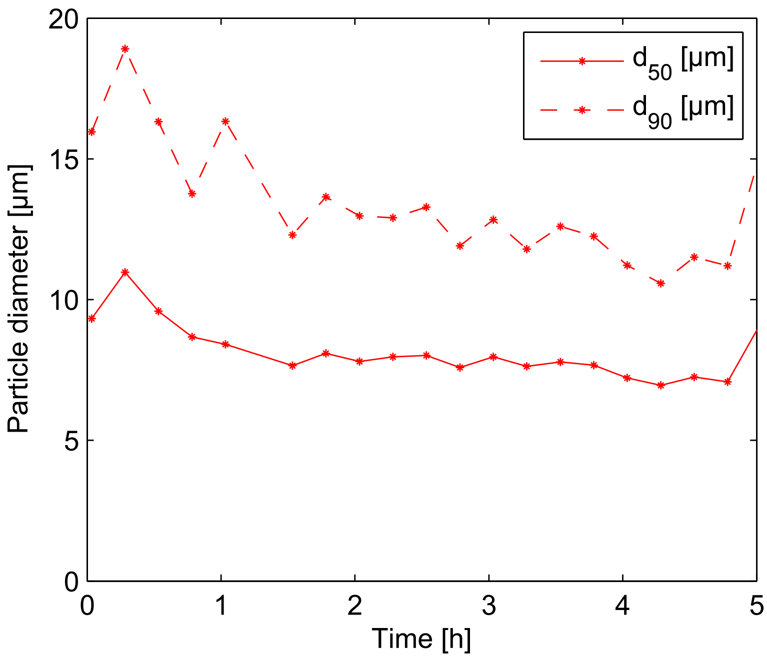

Fig. 6. Measured median diameter d_{50} and d_{90} of the particles over a time of approx. 5 h at the center of the cross section.

ESURFD
1, 437–481, 2013

Flocculation processes and sedimentation of fine sediments

I. Klassen et al.

ESURFD
1, 437–481, 2013

Flocculation processes and sedimentation of fine sediments

I. Klassen et al.

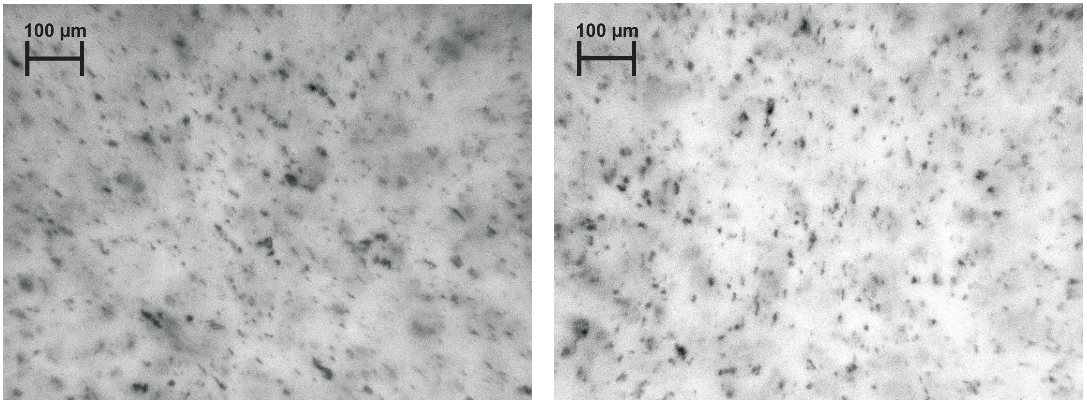

Fig. 7. Pictures of the particles, captured by the Aello In-Line microscope (left: d_{50} = 11 µm, right: d_{50} = 7.6 µm).

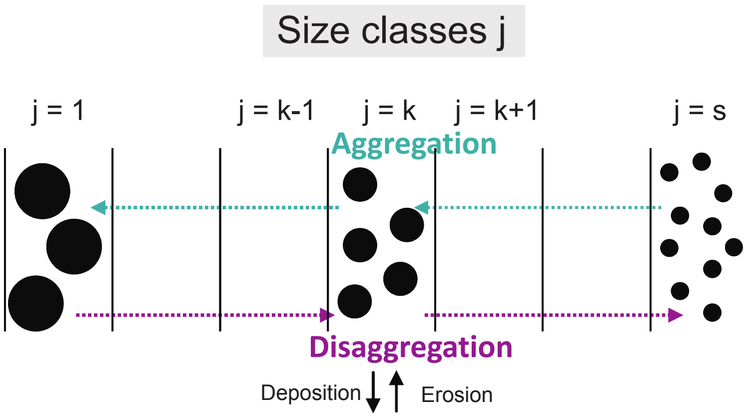

Fig. 8. Sediment mass fluxes between size classes by aggregation or disaggregation and deposition/erosion (McAnally, 1999; modified).

ESURFD
1, 437–481, 2013

Flocculation processes and sedimentation of fine sediments

I. Klassen et al.

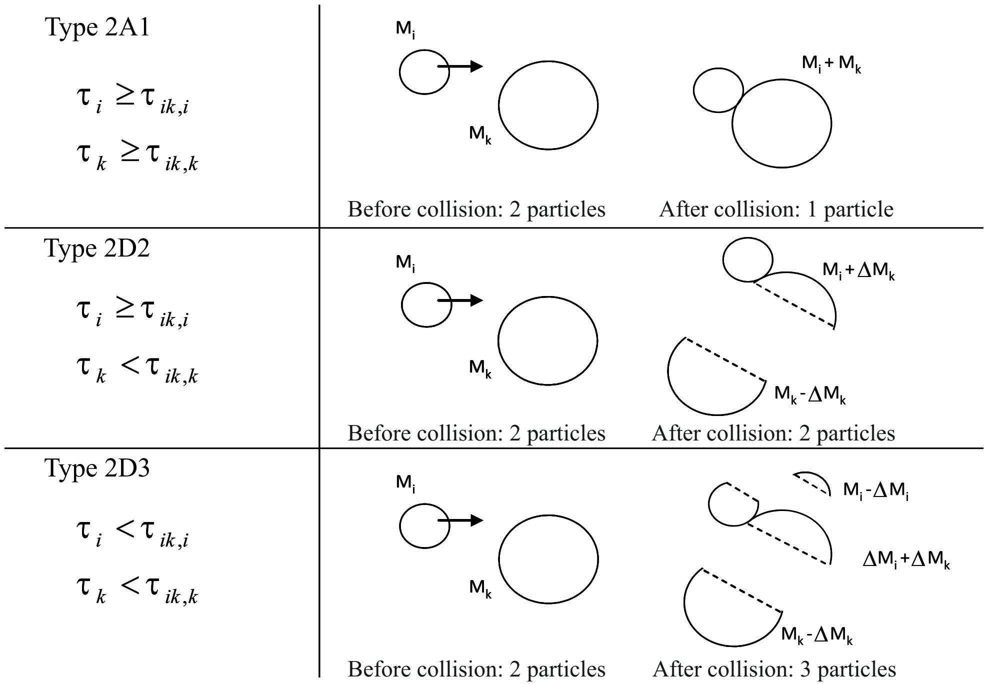

Fig. 9. Collision outcomes depending on the strength of the particles compared with the collision induced forces (McAnally, 1999; modified).

ESURFD
1, 437–481, 2013
Flocculation processes and sedimentation of fine sediments
I. Klassen et al.

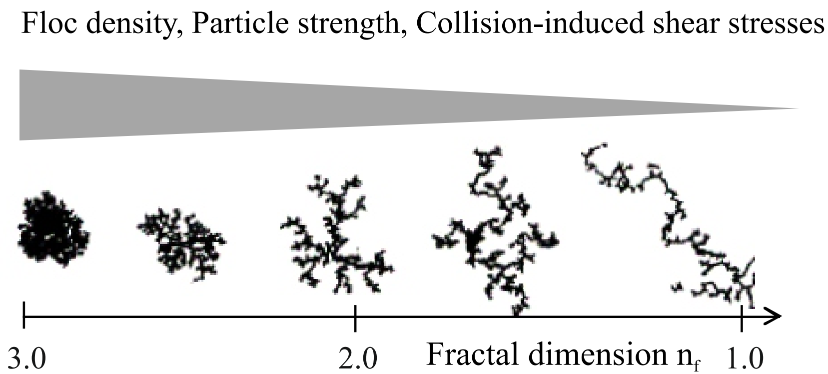

Fig. 10. Variable fractal dimension n_f ranging from n_f = 1.0 for large and fragile flocs to n_f = 3.0 for small and compact particles.

ESURFD
1, 437–481, 2013

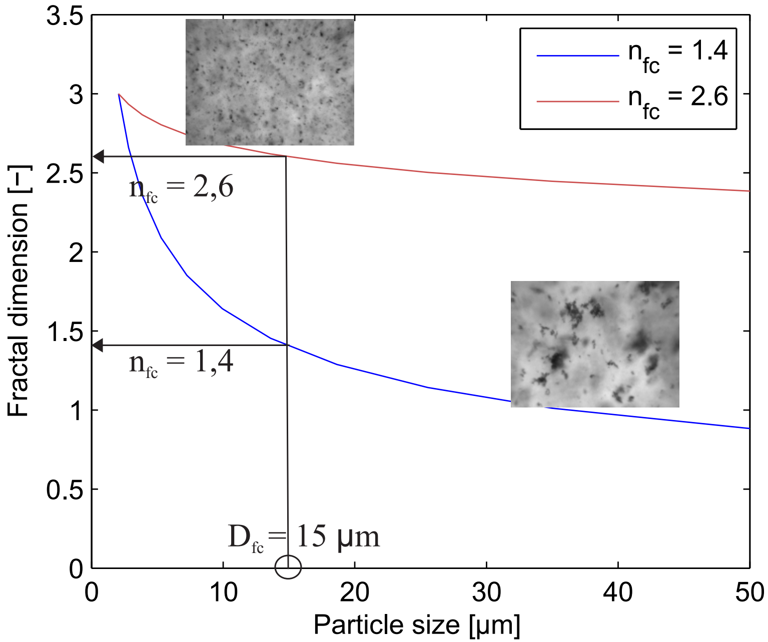

Fig. 11. Calculated variable fractal dimension n_f depending on the characteristic floc size D_{f_c} and the characteristic fractal dimension n_{f_c}.

ESURFD
1, 437–481, 2013

Flocculation processes and sedimentation of fine sediments

I. Klassen et al.

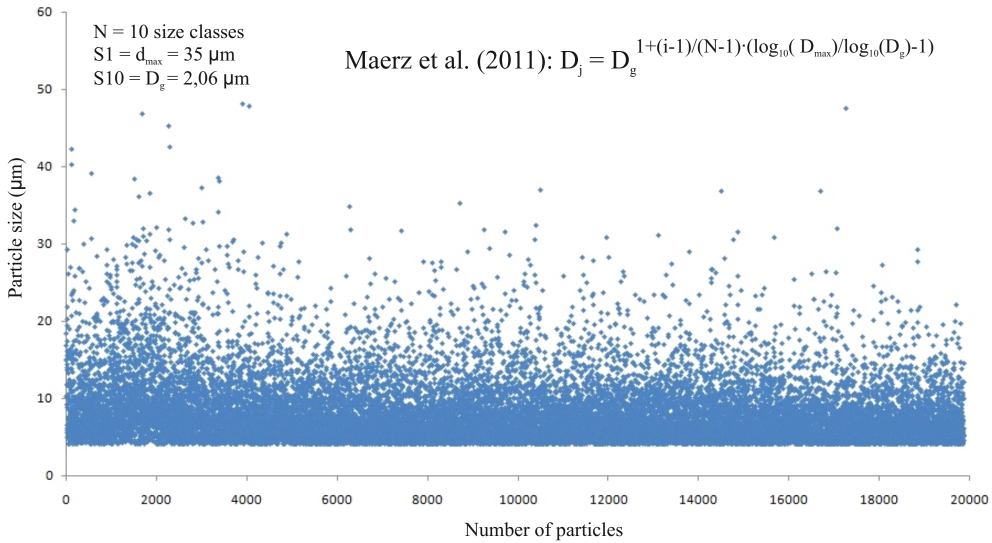

Fig. 12. All measured particle sizes in the first 5 h of the experiment.

ESURFD
1, 437–481, 2013

Title Page
Abstract | Introduction
Conclusions | References
Tables | Figures
◀| |▶
◀ ▶
Back | Close
Full Screen / Esc
Printer-friendly Version
Interactive Discussion

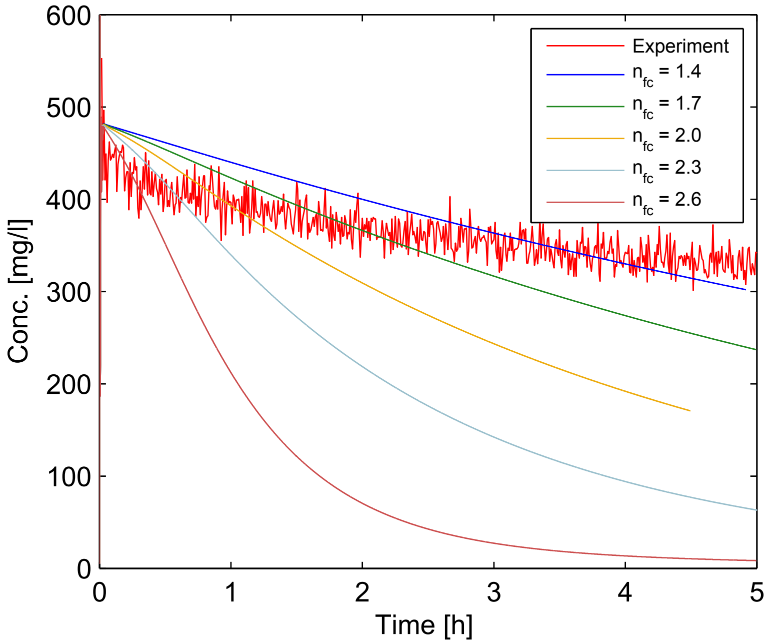

Fig. 13. Measured concentration (red, jagged line) and calculated concentrations by using different characteristic fractal dimensions n_{f_c} (= 1.4, 1.7, 2.0, 2.3 and 2.6).

Discussion Paper | Discussion Paper | Discussion Paper | Discussion Paper |

ESURFD
1, 437–481, 2013

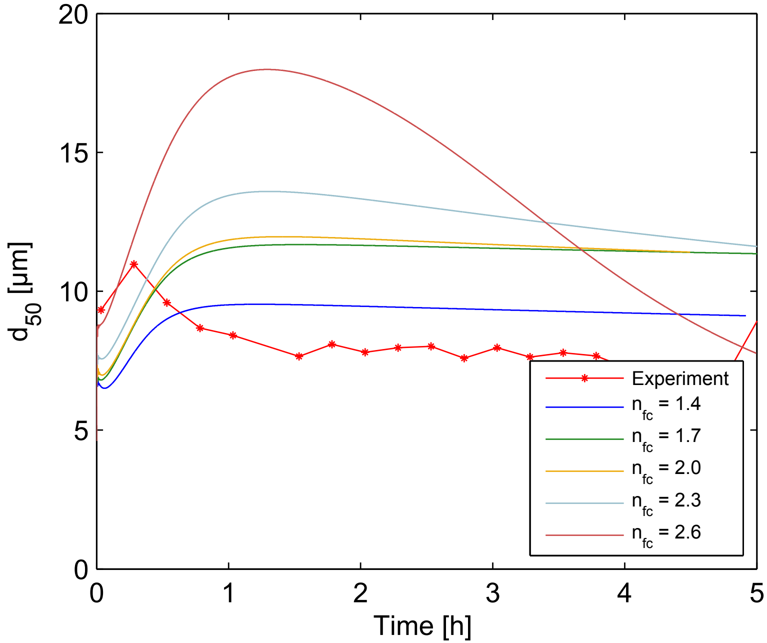

Fig. 14. Measured median diameter (red, dashed line) and calculated median floc diameter by using different characteristic fractal dimensions n_{f_c} (= 1.4, 1.7, 2.0, 2.3 and 2.6).

ESURFD
1, 437–481, 2013

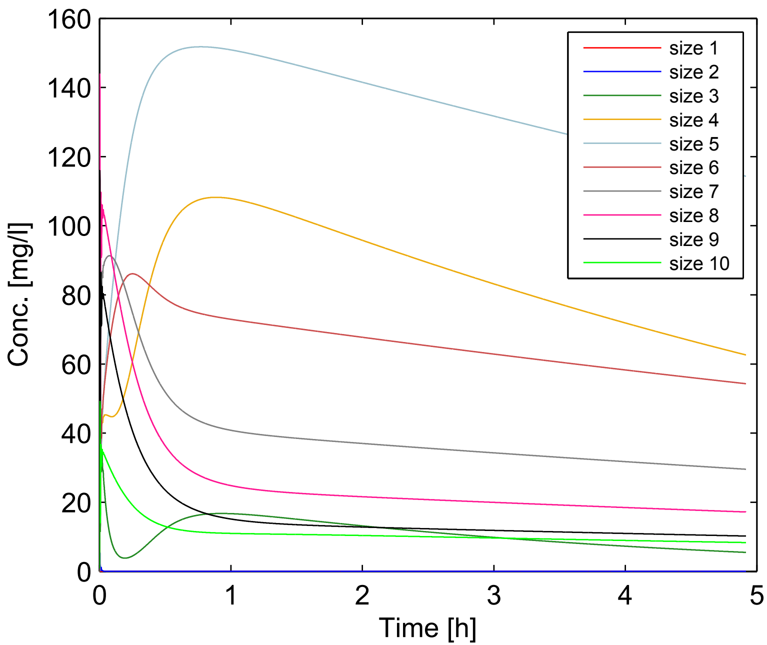

Fig. 15. Temporal development of the concentrations of each particle size class due to aggregation, break-up and deposition (n_{f_c} = 1.4, D_{f_c} = 15 µm).

ESURFD
1, 437–481, 2013

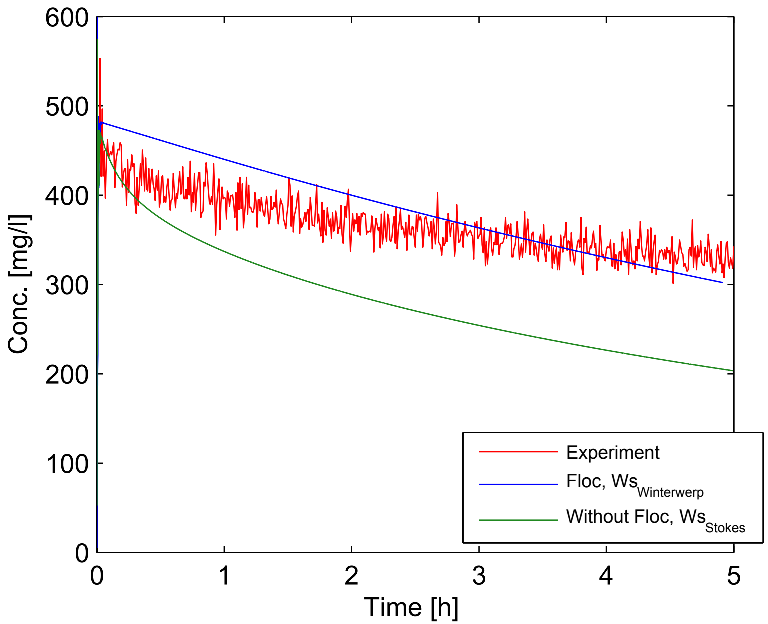

Fig. 16. Measured concentration (= red, jagged line) and calculated concentration by using the flocculation algorithm ($n_{f_c} = 1.4$, $D_{f_c} = 15\,\mu m$) and the settling velocity by Winterwerp (1998) (= blue line) and by excluding flocculation processes and using the settling velocity based on Stokes (1850) (= green line).

ESURFD
1, 437–481, 2013

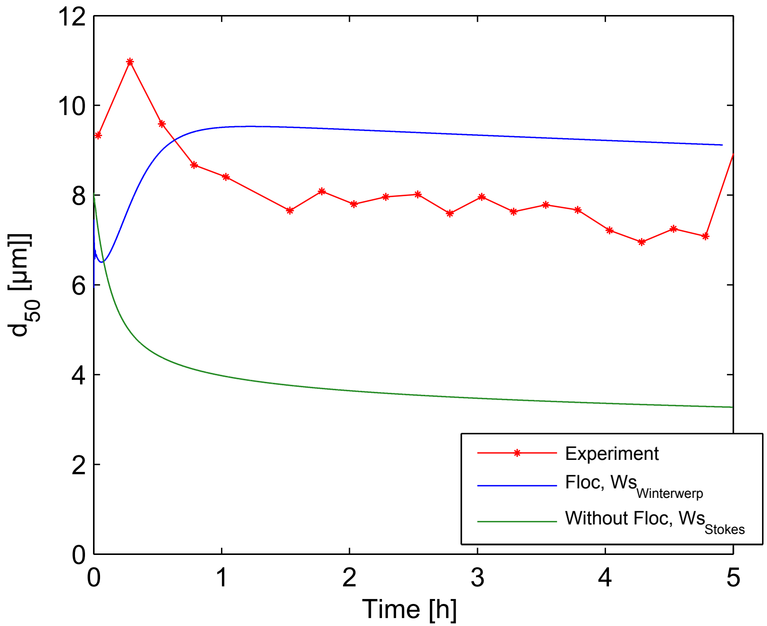

Fig. 17. Measured median diameter (red, dashed line) and calculated median floc diameter by using the flocculation algorithm ($n_{f_c} = 1.4$, $D_{f_c} = 15\,\mu m$) and the settling velocity by Winterwerp (1998) (= blue line) and by excluding flocculation processes and using the settling velocity based on Stokes (1850) (= green line).

ESURFD
1, 437–481, 2013

Flocculation processes and sedimentation of fine sediments

I. Klassen et al.

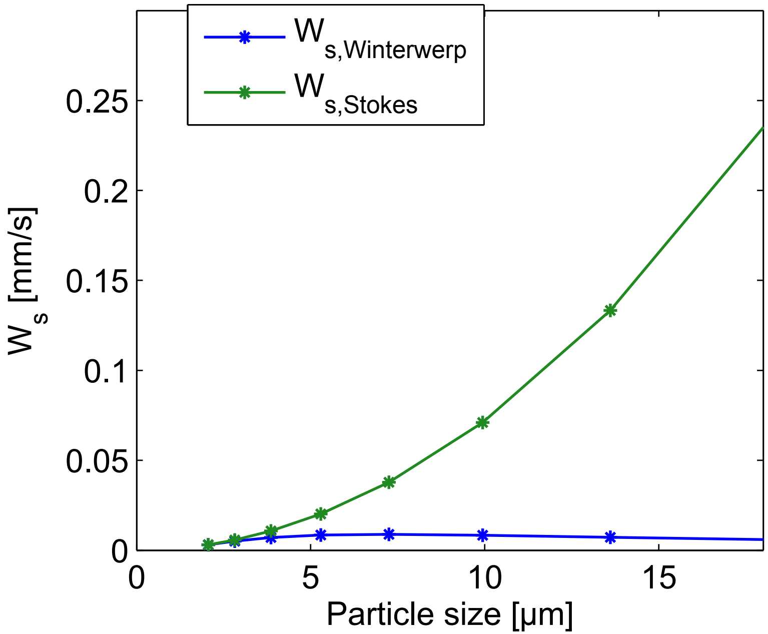

Fig. 18. Calculated settling velocity depending on the floc size by using Winterwerp's formula (blue line) or Stokes equation (green line).

ESURFD
1, 437–481, 2013

Flocculation processes and sedimentation of fine sediments

I. Klassen et al.